

We are IntechOpen, the world's leading publisher of Open Access books Built by scientists, for scientists

6,900

Open access books available

186,000

International authors and editors

200M

Downloads

Our authors are among the

154

Countries delivered to

TOP 1%

most cited scientists

12.2%

Contributors from top 500 universities



WEB OF SCIENCE™

Selection of our books indexed in the Book Citation Index
in Web of Science™ Core Collection (BKCI)

Interested in publishing with us?
Contact book.department@intechopen.com

Numbers displayed above are based on latest data collected.
For more information visit www.intechopen.com



Natural Circulation in Single and Two Phase Thermosyphon Loop with Conventional Tubes and Minichannels

Henryk Bieliński and Jarosław Mikielwicz

*The Szewalski Institute of Fluid-Flow Machinery, Polish Academy of Sciences,
Fiszera 14, 80-952 Gdańsk,
Poland*

1. Introduction

The primary function of a natural circulation loop (i.e. thermosyphon loop) is to transport heat from a source to a sink. Fluid flow in a thermosyphon loop is created by the buoyancy forces that evolve from the density gradients induced by temperature differences in the heating and cooling sections of the loop. An advanced thermosyphon loop consists of the evaporator, where the working liquid boils; and the condenser, where the vapour condenses back to liquid; the riser and the downcomer connect these two exchangers. Heat is transferred as the vaporization heat from the evaporator to the condenser. The thermosyphon is a passive heat transfer device, which makes use of gravity for returning the liquid to the evaporator. Thermosyphons are less expensive than other cooling devices because they feature no pump.

There are numerous engineering applications for thermosyphon loops such as, for example, solar water heaters, thermosyphon reboilers, geothermal systems, nuclear power plants, emergency cooling systems in nuclear reactor cores, electrical machine rotor cooling, gas turbine blade cooling, thermal diodes and electronic device cooling. The thermal diode is based on natural circulation of the fluid around the closed-loop thermosyphon (Bieliński & Mikielwicz, 1995, 2001), (Chen, 1998). The closed-loop thermosyphon is also known as a "liquid fin" (Madejski & Mikielwicz, 1971).

Many researchers focused their attention on the single-phase loop thermosyphons with conventional tubes, and the toroidal and the rectangular geometry of the loop. For example, Zvirin (Zvirin, 1981) presented results of theoretical and experimental studies concerned with natural circulation loops, and modeling methods describing steady state flows, transient and stability characteristics. Greif (Greif, 1988) reviewed basic experimental and theoretical work on natural circulation loops. Misale (Misale et al., 2007) reports an experimental investigations related to rectangular single-phase natural circulation mini-loop. Ramos (Ramos et al., 1985) performed the theoretical study of the steady state flow in the two-phase thermosyphon loop with conventional tube. Vijayan (Vijayan et al., 2005) compared the dynamic behaviour of the single-phase and two-phase thermosyphon loop with conventional tube and the different displacement of heater and cooler. The researcher found that the most stable configuration of the thermosyphon loop with conventional tube is the one with both vertical cooler and heater.

In the case of closed rectangular and toroidal loops with conventional tube, particular attention has to be devoted to both transient and steady state flows as well as to stability analysis of the system under various heating and cooling conditions.

The purpose of this chapter is to present a detailed analysis of heat transfer and fluid flow in a new generalized model of thermosyphon loop and its different variants. Each individual variant can be analyzed in terms of single- and two-phase flow in the thermosyphon loop with conventional tubes and minichannels. The new empirical correlations for the heat transfer coefficient in flow boiling and condensation, and two-phase friction factor in diabatic and adiabatic sectors in minichannels and conventional tube, are used to simulate the two-phase flow and heat transfer in the thermosyphon loop. The analysis of the thermosyphon loop is based on the one-dimensional model, which includes mass, momentum and energy balances.

2. A generalized model of the thermosyphon loop

A schematic diagram of a one-dimensional generalized model of the thermosyphon loop is shown in Fig. 1.

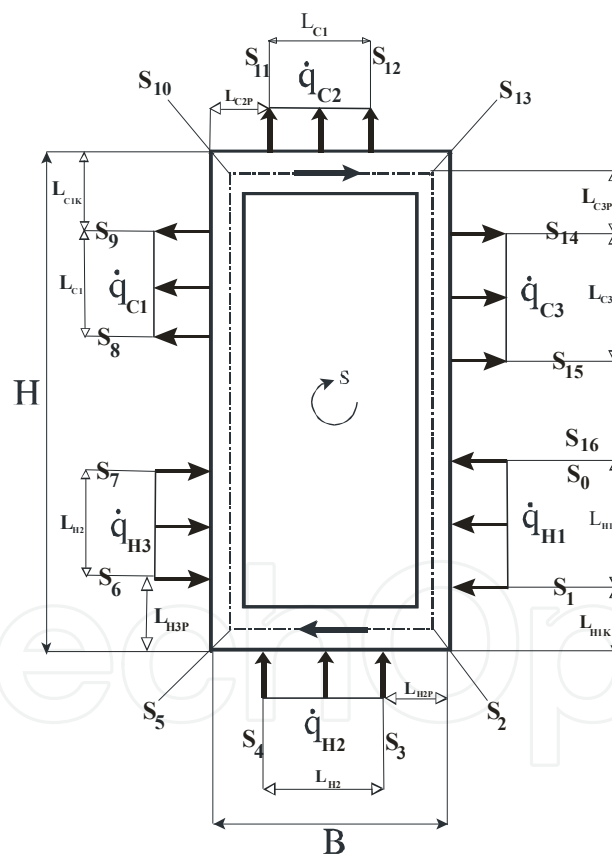


Fig. 1. A schematic diagram of a one-dimensional generalized model of the thermosyphon loop.

The loop has a provision for selecting one or two or three of the heat sources at any location, in the bottom horizontal pipe or in the vertical leg; similarly, the heat sink can be chosen in the top horizontal pipe or in the vertical leg. Therefore, any combination of heaters and coolers can be analyzed. The constant heat fluxes \dot{q}_H and \dot{q}_C are applied in the cross-

section area per heated and cooled length: L_H and L_C . The heated and cooled parts of the thermosyphon loop are connected by perfectly insulated channels. The coordinate s along the loop and the characteristic geometrical points on the loop are marked with s_j , as shown in Fig. 1. The total length of the loop is denoted by L , the cross-section area of the channel by A and the wetted perimeter by U . Thermal properties of fluid: ρ - density, c_p - heat capacity of constant pressure, λ - thermal conductivity.

The following assumptions are used in the theoretical model of natural circulation in the closed loop thermosyphon:

1. thermal equilibrium exists at any point of the loop,
2. incompressibility because the flow velocity in the natural circulation loop is relatively low compared with the acoustic speed of the fluid under current model conditions,
3. viscous dissipation in fluid is neglected in the energy equations,
4. heat losses in the thermosyphon loop are negligible,
5. $(D/L) \ll 1$; one-dimensional models are used and the flow is fully mixed. The velocity and temperature variation at any cross section is therefore neglected,
6. heat exchangers in the thermosyphon loop can be equipped by conventional tubes or minichannels,
7. fluid properties are constants, except density in the gravity term,
8. single- and two-phase fluid can be selected as the working fluid,
 - a. if the Boussinsq approximation is valid for a single-phase system, then density is assumed to vary as $\rho = \rho_0 \cdot [1 - \beta \cdot (T - T_0)]$ in the gravity term where $\beta = \frac{1}{\nu_0} \cdot \left(\frac{\partial \nu}{\partial T} \right)_p$ (ν - specific volume, "0" is the reference of steady state),
 - b. for the calculation of the frictional pressure loss in the heated, cooled and adiabatic two-phase sections, the two-phase friction factor multiplier $R = \phi_{L0}^2$ is used; the density in the gravity term can be approximated as follows: $\rho = \alpha \cdot \rho_V + (1 - \alpha) \cdot \rho_L$, where α is a void fraction,
 - c. homogeneous model or separate model can be used to evaluate the friction pressure drop of two phase flow,
 - d. quality of vapor in the two-phase regions is assumed to be a linear function of the coordinate around the loop,
9. the effect of superheating and subcooling are neglected,

Under the above assumptions, the governing equations for natural circulation systems can be written as follows:

- conservation of mass:

$$\frac{\partial \rho}{\partial \tau} + \frac{\partial}{\partial s}(\rho \cdot w) = 0; \tag{1}$$

where τ - time, w - velocity.

- conservation of momentum:

$$\rho \cdot \left(\frac{\partial w}{\partial \tau} + w \cdot \frac{\partial w}{\partial s} \right) = - \frac{\partial p}{\partial s} + \varepsilon \cdot \rho \cdot \tilde{g} - \tau_w \cdot \frac{U}{A}; \tag{2}$$

where $\varepsilon = 0$ for $\vec{e} \perp \vec{g}$; $\varepsilon = (+1)$ for $\vec{e} \uparrow \wedge \vec{g} \downarrow$; $\varepsilon = (-1)$ for $\vec{e} \downarrow \wedge \vec{g} \downarrow$; $\tilde{g} = \vec{e} \circ \vec{g} = 1 \cdot g \cdot \cos(\vec{e}, \vec{g})$; $|\vec{g}| = g$; $|\vec{e}| = 1$; and \vec{e} is a versor of the coordinate around the loop, and τ_w - wall shear stress.

In order to eliminate the pressure gradient and the acceleration term, the momentum equation in Eq. (2) is integrated around the loop $\oint \left(\frac{\partial p}{\partial s} \right) ds = 0$.

- conservation of energy:

$$\frac{\partial T}{\partial \tau} + w \cdot \frac{\partial T}{\partial s} = a_0 \cdot \frac{\partial^2 T}{\partial s^2} \begin{cases} +0 & \text{for adiabatic section} \\ -\frac{q_C \cdot U}{c_{p0} \cdot \rho_0 \cdot A} & \text{for cooled section} \\ +\frac{\dot{q}_H \cdot U}{c_{p0} \cdot \rho_0 \cdot A} & \text{for heated section} \end{cases} \quad (3)$$

where $a_0 = \frac{\lambda_0}{\rho_0 \cdot c_{p0}}$ - thermal diffusivity,

The flow in natural circulation systems which is driven by density distribution is also known as a gravity driven flow or thermosyphonic flow. In such flows, the momentum and the energy equations are coupled and for this reason they need to be simultaneously solved (Mikielewicz, 1995).

3. Thermosyphon loop Heated from below Horizontal side and Cooled from upper Horizontal side (HHCH).

In this paper, we present the case of the onset of motion of the single-phase fluid from a rest state, which occurs only for the (HHCH) variant. We have assumed that: $\dot{q}_C = \alpha_C \cdot (T - T_0)$. The heat transfer coefficient between the wall and environment α_C and the temperature of the environment T_0 are constant.

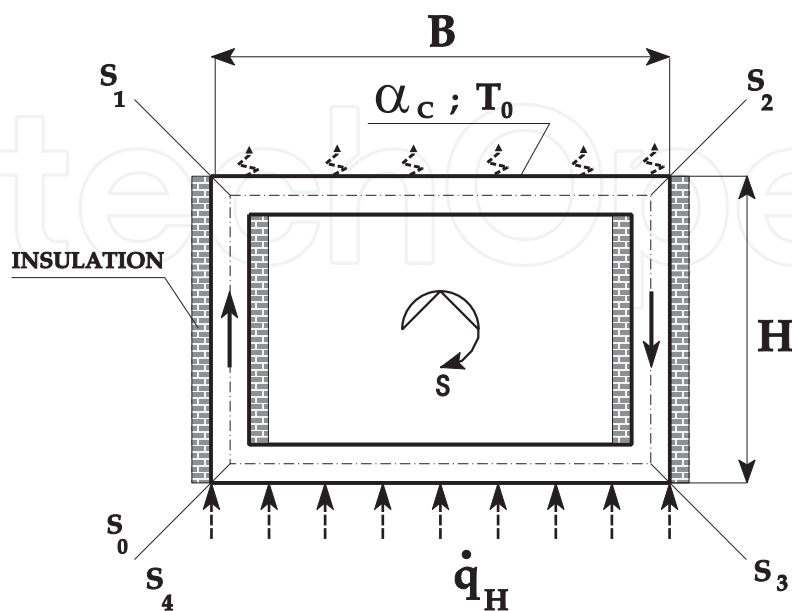


Fig. 2. The variant of HHCH.

The above governing equations can be transformed to their dimensionless forms by the following scaling:

$$\tau^+ = (a_0 \cdot \tau) / L^2; \quad s^+ = s / L; \quad \dot{m}^+ = (\dot{m} \cdot L) / (a_0 \cdot \rho_0 \cdot A); \quad T^+ = \frac{\lambda_0 \cdot (A / U_H) \cdot (T - T_0)}{(\dot{q}_H \cdot L^2)}; \quad (4)$$

The dimensionless momentum equation and the energy equation at the steady state for the thermosyphon loop heated from below can be written as follows:

- momentum equation (with: $K_j = s_j / L$;)

$$\dot{m}^+ = (Ra)^{**} \cdot \left(\int_0^{K_1} T^+ ds^+ - \int_{K_2}^{K_3} T^+ ds^+ \right); \quad (5)$$

- energy equation

$$\dot{m}^+ \frac{dT^+}{ds^+} = \frac{d^2 T^+}{ds^{+2}} \begin{cases} +0 & \text{insulated sections} \\ -(Bi)^{**} \cdot T^+ & \text{for cooling section} \\ +1 & \text{heater section} \end{cases} \quad (6)$$

- with boundary conditions

$$\begin{aligned} T_{A1}^+(0) &= T_H^+(1); \quad T_{A1}^+(K_1) = T_C^+(K_1); \quad T_C^+(K_2) = T_{A2}^+(K_2); \quad T_{A2}^+(K_3) = T_H^+(K_3); \\ \frac{dT_{A1}^+}{ds^+} \Big|_{s^+=0} &= \frac{dT_H^+}{ds^+} \Big|_{s^+=1}; \quad \frac{dT_{A1}^+}{ds^+} \Big|_{s^+=K_1} = \frac{dT_C^+}{ds^+} \Big|_{s^+=K_1}; \\ \frac{dT_C^+}{ds^+} \Big|_{s^+=K_2} &= \frac{dT_{A2}^+}{ds^+} \Big|_{s^+=K_2}; \quad \frac{dT_{A2}^+}{ds^+} \Big|_{s^+=K_3} = \frac{dT_H^+}{ds^+} \Big|_{s^+=K_3}; \end{aligned} \quad (7)$$

The parameters appearing in the momentum and the energy equations are the modified Biot, Rayleigh and Prandtl numbers.

$$(Bi)^{**} = \frac{\alpha_C \cdot U_C \cdot L^2}{\lambda_0 \cdot A}; \quad (Ra)^{**} = \frac{g \cdot \beta_0 \cdot L^3 \cdot (\dot{q}_H / \lambda_0) \cdot A \cdot U_H}{\nu_0 \cdot a_0 \cdot 2 \cdot U^2}; \quad (Pr)^{**} = 2 \cdot L^2 \cdot \left(\frac{U}{A} \right)^2 \cdot \left(\frac{\nu_0}{a_0} \right); \quad (8)$$

For the discussed case of laminar steady-state flow the dimensionless distributions of temperature around the loop can be obtained analytically from Eq. (6). Working fluid was the distilled water. The results of calculations are presented in Fig. 3.

It has been found that the Biot number has an influence on temperature and mass flow rate in the laminar flow. The results are shown in Figs. 3 and 4.

Substitution of the temperature distributions into the dimensionless equation of motion for the steady-state yields the relation for the dimensionless flow rate for laminar flow.

The presented numerical calculations are based on our new method for solution of the problem for the onset of motion in the fluid from the rest. Conditions for the onset of motion

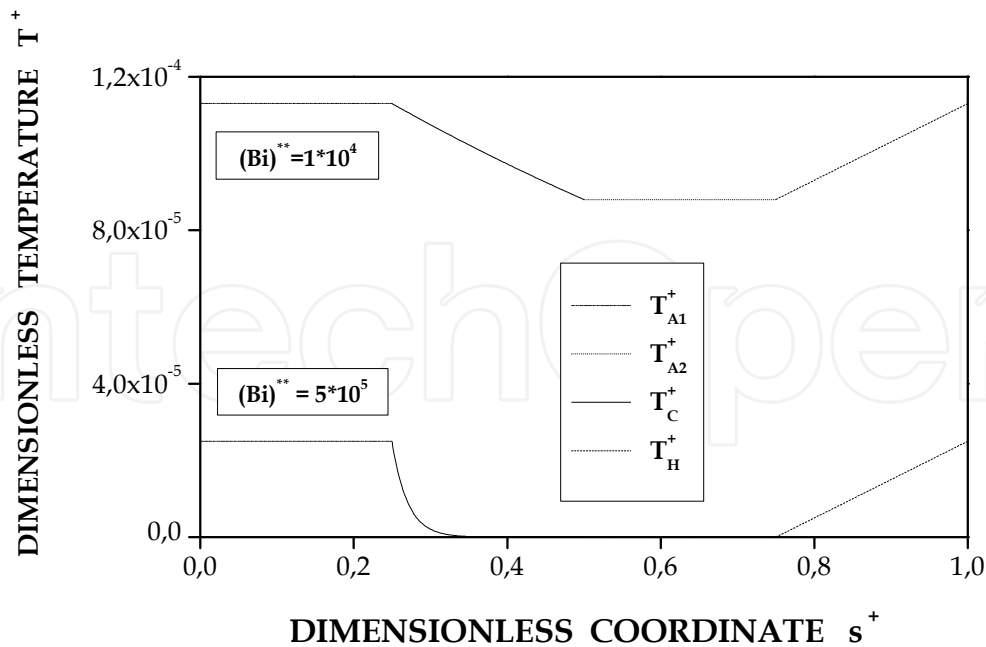


Fig. 3. The effect of Biot number on temperatures in laminar steady-state flow (HHCH).

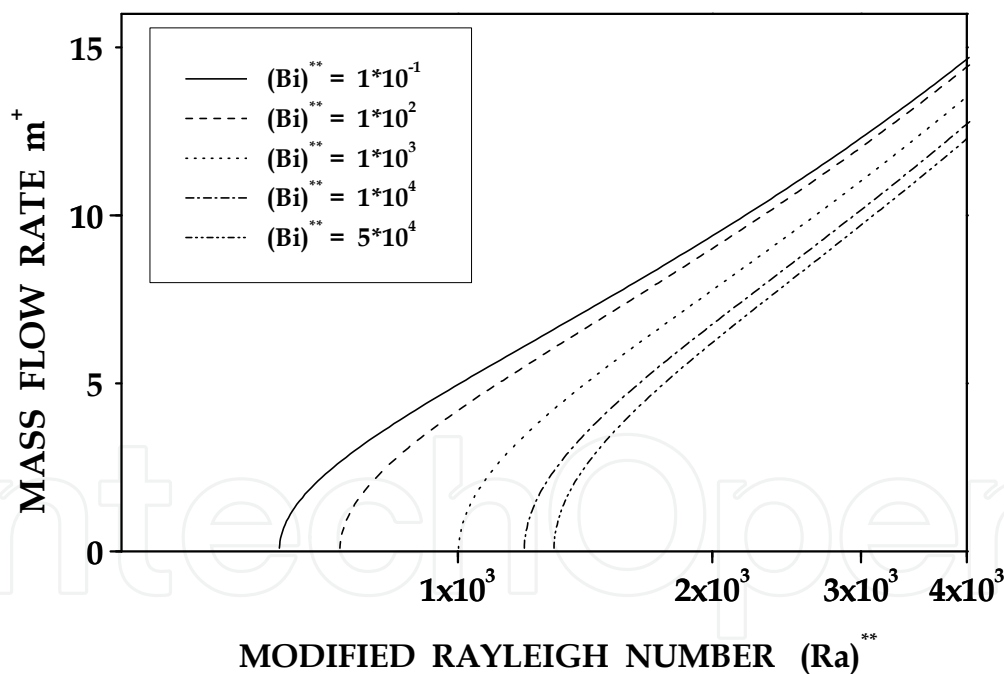


Fig. 4. The dimensionless mass flow rate \dot{m}^+ versus modified Rayleigh number $(Ra)^{**}$ with the modified Biot number $(Bi)^{**}$ used as a fixed parameter (HHCH).

in the thermosyphon can be determined by considering the steady solutions with circulation for the limiting case of $\dot{m}_1^+ \rightarrow 0$. The analysis was based on the equations of motion and energy for the steady-state conditions. The heat conduction term has to be taken into account in this approach because the heat transfer due to conduction is becoming an increasingly important factor for decreasing mass flow rates.

It is shown that the geometrical and thermal parameters have an influence on the problem of global flow initiation from the rest (Figs. 4, 5 and 6).

Fig. 5 illustrates that the larger Biot numbers correspond to larger values of the critical Rayleigh number.

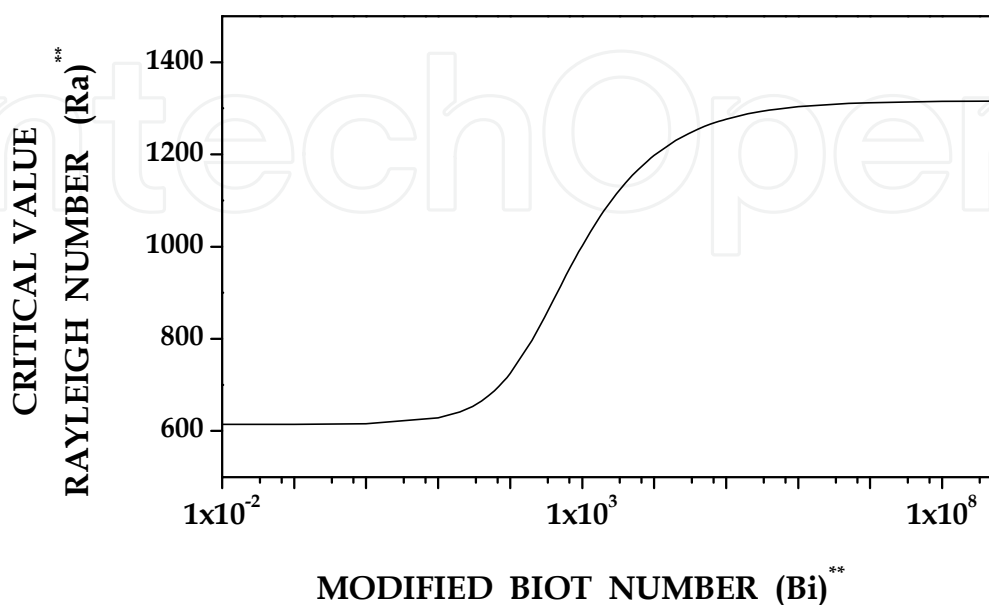


Fig. 5. The critical value of the modified Rayleigh number $(Ra)^{**}$ versus modified Biot number $(Bi)^{**}$ (HHCH).

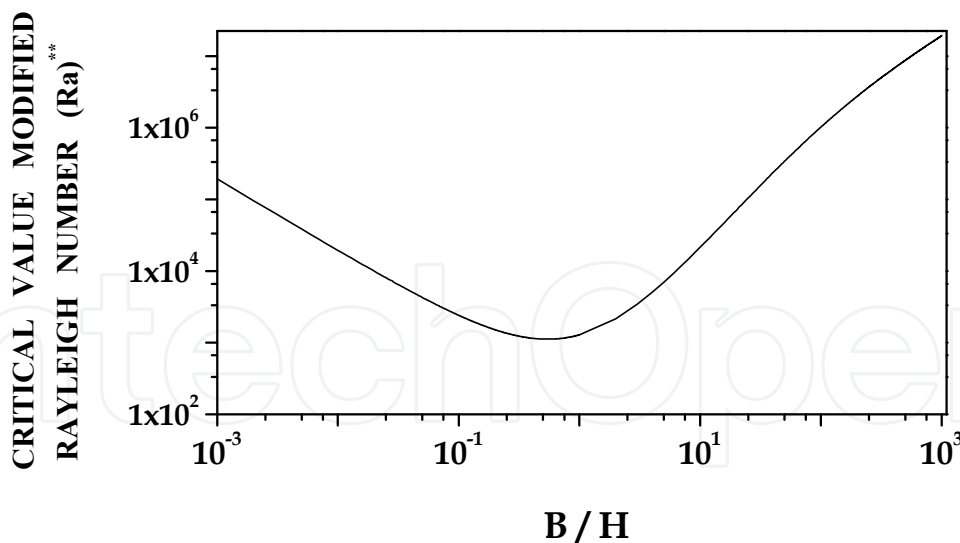


Fig. 6. The critical value of the modified Rayleigh number $(Ra)^{**}$ versus B/H ratio (HHCH).

It has been found that the minimum of the critical modified Rayleigh number $(Ra)^{**} = 1121$, with $(Bi)^{**} = 2 \times 10^5$, appears for $B/H = 0.544$.

The stability analysis shows that the loop heated from one side and cooled from the other one asymmetrically with respect to the gravity force is always unstable and any temperature gradient due to heating or cooling results in the onset of flow circulation.

4. Thermosyphon loop Heated from the lower part of Vertical side and Cooled from the upper part of the opposite Vertical side (HVCV).

The thermosyphon loop heated from the lower part of vertical leg and cooled from the upper part of the opposite vertical leg (HVCV) is chosen as an example to present the analysis of two-phase flow in conventional tubes. The Stomma (Stomma, 1979) correlation describing the void fraction, the Friedel (Friedel, 1979) correlation for the friction pressure drop of two-phase flow in adiabatic region, the Müller-Steinhagen & Heck (Müller-Steinhagen & Heck, 1986) correlation for the friction pressure drop of two-phase flow in diabatic region and the Mikielewicz correlation for the flow boiling heat transfer coefficient in conventional channels (Mikielewicz et al., 2007) are used to calculate two phase flow in the thermosyphon loop equipped with conventional tubes. Freon R-11 was chosen as a working fluid in the thermosyphon device. A schematic diagram of the analysed thermosyphon loop (HVCV) is shown in Fig. 7.

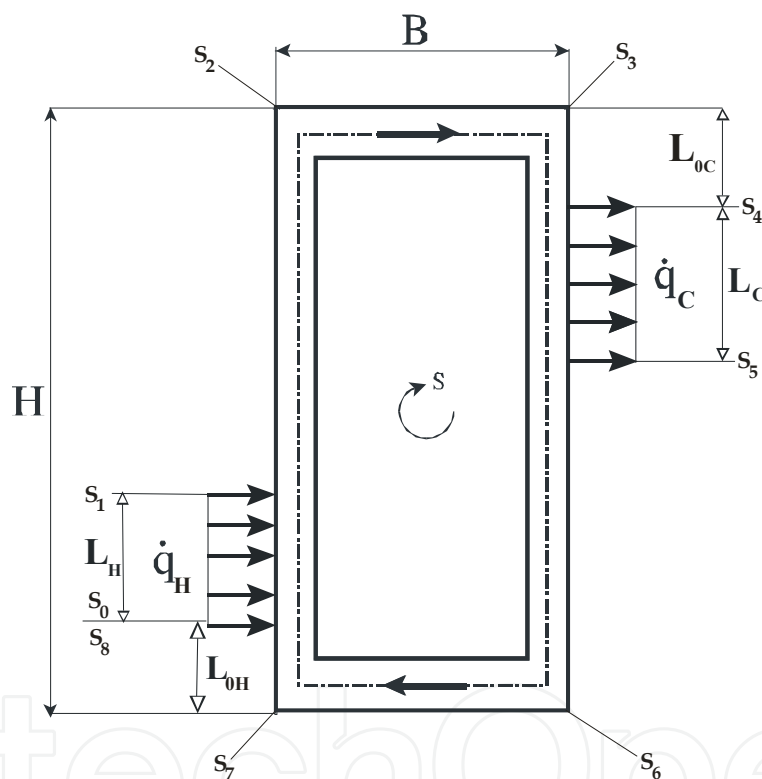


Fig. 7. The thermosyphon loop heated from the lower part of vertical side and cooled from the upper part of the opposite vertical side (HVCV).

After integrating the gravitational term in the momentum equation (2) around the loop, we obtain

$$\begin{aligned} \oint \left\{ \varepsilon \cdot g \cdot \left[(1 - \alpha) \cdot \rho_L + \alpha \cdot \rho_V \right] \right\} ds = \\ = g \cdot (\rho_V - \rho_L) \times \left\{ \left[(s_2 - s_1) - (s_4 - s_3) \right] \cdot \bar{\alpha}_{\langle s_1; s_4 \rangle} + (s_1 - s_0) \cdot \bar{\alpha}_{\langle s_0; s_1 \rangle} - (s_5 - s_4) \cdot \bar{\alpha}_{\langle s_4; s_5 \rangle} \right\}; \end{aligned} \quad (9)$$

$$\text{where } \bar{\alpha}_{\langle s_P; s_K \rangle} = \frac{1}{(s_K - s_P)} \cdot \int_{s_P}^{s_K} \alpha_{\langle s_P; s_K \rangle}(s) ds .$$

The Stomma empirical correlation (Stomma, 1979) for the void fraction at low pressures is applied in the form

$$\alpha^{STOMMA} = 1 - \frac{[(\alpha_{HOM})^2 - (x)^2]}{2 \cdot \left[\ln\left(\frac{1-x}{1-\alpha_{HOM}}\right) - (\alpha_{HOM} - x) \right]} \quad (10)$$

where $\alpha_{HOM} = \frac{1}{1 + \frac{1-x}{x} \cdot \left(\frac{\rho_V}{\rho_L}\right)}$. (Subscripts: V - vapour, L - liquid, HOM - homogeneous).

The following additional assumptions are made in this study (HVCV): a) flows of liquid and vapour phases in the two-phase regions are both turbulent and flow of liquid in single phase region is also turbulent, b) friction coefficient is constant in each region of the loop and the frictional component of the pressure gradient in two-phase regions was calculated according to the two-phase separate model. Due to the friction of fluid, the pressure losses in two-phase regions can be calculated as

$$\frac{U}{A} \cdot \tau_w = \left(\frac{-dp}{ds}\right)_{2p} = R \cdot \left(\frac{-dp}{ds}\right)_{L0} \quad (11)$$

where: $\left(\frac{dp}{ds}\right)_{L0} = \frac{2 \cdot f_{L0}^{Chur} \cdot (\dot{G})^2}{D \cdot \rho_L}$ is the liquid only frictional pressure gradient calculated for the total liquid mass velocity, $\dot{G} = \rho \cdot w$, f_{L0}^{Chur} is friction factor of the fluid (Churchill, 1977). The local two-phase friction coefficient in two-phase adiabatic region was calculated using the Friedel formula (Friedel, 1979):

$$\left(\frac{dp}{ds}\right)_{2f,Frict}^{FRIEDEL} = \Phi_{L0}^2 \cdot \left(\frac{dp}{ds}\right)_{L0} ; \quad (12)$$

where

$$\Phi_{L0}^2 = E + \frac{3.24 \cdot F \cdot H}{(Fr)^{0.045} \cdot (We)^{0.035}} ;$$

and

$$E = (1-x)^2 + x^2 \cdot \frac{\rho_L \cdot f_{V0}}{\rho_V \cdot f_{L0}} ; F = (x)^{0.78} \cdot (1-x)^{0.224} ; H = \left(\frac{\rho_L}{\rho_V}\right)^{0.91} \cdot \left(\frac{\mu_V}{\mu_L}\right)^{0.19} \cdot \left(1 - \frac{\mu_V}{\mu_L}\right)^{0.7} ;$$

and (σ - surface tension)

$$(Fr) = \frac{(\dot{G})^2}{g \cdot D \cdot (\rho_{HOM})^2} ; (We) = \frac{(\dot{G})^2 \cdot D}{(\rho_{HOM}) \cdot \sigma} ;$$

The local two-phase friction coefficient in two-phase diabatic regions was calculated using the Müller-Steinhagen & Heck formula (Müller-Steinhagen & Heck, 1986)

$$\left(\frac{dp}{ds}\right)_{2f,Frict}^{M-S} = F \cdot (1-x)^{\frac{1}{3}} + B \cdot x^3 ; \quad (13)$$

where

$$F = A + 2 \cdot x \cdot (B - A) ; \quad A = \left(\frac{dp}{ds}\right)_{L0} ; \quad B = \left(\frac{dp}{ds}\right)_{V0} ;$$

After integrating the friction term in Eq. (2) around the loop, we obtain

$$\oint \left(\frac{U}{A} \cdot \tau_w\right) ds = \left(\frac{dp}{ds}\right)_{L0} \cdot \left\{ (s_1 - s_0) \cdot \bar{R}_{(s_0;s_1)} + (s_4 - s_1) \cdot \bar{R}_{(s_1;s_4)} + (s_5 - s_4) \cdot \bar{R}_{(s_4;s_5)} + (s_8 - s_5) \right\}; \quad (14)$$

$$\text{where: } \bar{R}_{(s_P;s_K)} = \frac{1}{(s_K - s_P)} \cdot \int_{s_P}^{s_K} R(s) ds .$$

Thus the momentum equation (2) for the two-phase thermosyphon loop (HVCV) can be written as

$$\left(\frac{dp}{ds}\right)_{L0} \cdot \left\{ (s_1 - s_0) \cdot \bar{R}_{(s_0;s_1)} + (s_4 - s_1) \cdot \bar{R}_{(s_1;s_4)} + (s_5 - s_4) \cdot \bar{R}_{(s_4;s_5)} + (s_8 - s_5) \right\} + g \cdot (\rho_V - \rho_L) \cdot \left\{ [(s_2 - s_1) - (s_4 - s_3)] \cdot \bar{\alpha}_{(s_1;s_4)} + (s_1 - s_0) \cdot \bar{\alpha}_{(s_0;s_1)} - (s_5 - s_4) \cdot \bar{\alpha}_{(s_4;s_5)} \right\} = 0 ; \quad (15)$$

The mass flux distributions \dot{G} versus heat flux \dot{q}_H for the steady-state conditions and for the conventional tube case, is shown in Fig. 8. Calculations were carried out also using the homogeneous model of two-phase flow. The working fluid was freon R11.

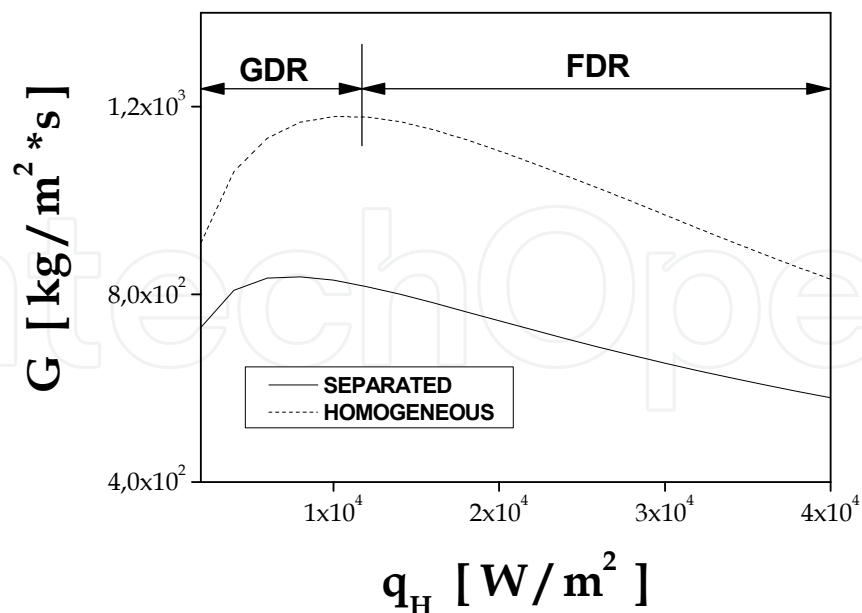


Fig. 8. Mass flux rate \dot{G} as a function of \dot{q}_H for homogeneous model and separate model of two-phase flow (HVCV), ($L=2$ [m], $D=0.08$ [m], $H=0.9$ [m], $B=0.1$ [m], $L_H=L_C=0.2$ [m], $L_{HP}=L_{CP}=0.05$ [m]).

Two flow regimes can be clearly identified in Fig. 8, namely GDR - gravity dominant regime and FDR - friction dominant regime. In the gravity dominant regime, for a small change in quality there is a large change in the void fraction and therefore density and buoyancy force. The increased buoyancy force can be balanced by a significant increase in the corresponding frictional force which is possible only at higher flow rates. As a result, the gravity dominant regime is characterized by an increase in the flow rate with heat flux \dot{q}_H . However, the continued conversion of high density water to low density steam due to increase in heat flux \dot{q}_H requires that the mixture velocity must increase resulting in the increase of the frictional force and hence a decrease in flow rate. Thus the friction dominant regime is characterized by a decrease in flow rate with increase in heat flux \dot{q}_H (Vijayan et al., 2005). As presented in Fig. 8 a comparison between two models of two-phase flow shows that the homogeneous and the separated flow models reveal relatively big differences.

4.1 The distributions of heat transfer coefficient in flow boiling.

The heat transfer coefficient in flow boiling in minichannels was calculated using the Mikielewicz general formula for conventional channels (Mikielewicz et al., 2007)

$$\frac{h_{TPB}^{JM}}{h_{REF}} = \sqrt{\left(R_{M-S}\right)^n + \frac{1}{1+P} \cdot \left(\frac{h_{PB}}{h_{REF}}\right)^2} ; \quad (16)$$

where

$$R_{M-S} = \left[1 + 2 \cdot \left(\frac{1}{f_1} - 1 \right) \cdot x \right] \cdot (1-x)^{\frac{1}{3}} + x^3 \cdot \frac{1}{f_{1z}} ;$$

$$\text{TUR} \Rightarrow n = 0.76 ; h_{REF} = 0.023 \cdot \frac{\lambda_L}{D} \cdot (\text{Re}_{L0})^{0.8} \cdot (\text{Pr}_L)^{\frac{1}{3}} ;$$

$$f_1^{\text{TUR}} = \left(\frac{\mu_L}{\mu_V} \right)^{0.25} \cdot \left(\frac{\rho_V}{\rho_L} \right) ; f_{1z}^{\text{TUR}} = \left(\frac{\mu_V}{\mu_L} \right)^{\frac{7}{15}} \cdot \left(\frac{c_{pL}}{c_{pV}} \right)^{\frac{1}{3}} \cdot \left(\frac{\lambda_L}{\lambda_V} \right)^{\frac{3}{2}} ;$$

$$P = 2.53 \times 10^{(-3)} \cdot (\text{Re}_{L0})^{1.17} \cdot (\text{Bo})^{0.6} \cdot (R_{M-S} - 1)^{(-0.65)} ;$$

$$h_{PB} = 55 \cdot \dot{q}^{0.67} \cdot M^{(-0.5)} \cdot \left(\frac{P_n}{P_{\text{CRIT}}} \right)^{0.12} \cdot \left[-\log_{10} \left(\frac{P_n}{P_{\text{CRIT}}} \right) \right]^{(-0.55)} ; (\text{Bo}) = \frac{\dot{q}}{\dot{G} \cdot r} ; (\text{Re}_{L0}) = \frac{\dot{G} \cdot d}{\mu_L} ;$$

For comparison purposes the heat transfer coefficient for flow boiling in minichannels was also calculated using the Liu and Winterton formula (Liu & Winterton, 1991):

$$h_{TPB}^{L-W} = \sqrt{\left(F \cdot h_{REF}\right)^2 + \left(S \cdot h_{PB}\right)^2} ; \quad (17)$$

where

$$F = \left[1 + x \cdot (\text{Pr}_L) \cdot \left(\frac{\rho_L}{\rho_V} - 1 \right) \right]^{0.35} ; S = \left[\frac{1}{\left(1 + 0.055 \cdot (F)^{0.1} \cdot (\text{Re}_{L0})^{1.16} \right)} \right] ; (\text{Fr}) = \frac{\dot{G}}{\rho_L^2 \cdot g \cdot D} ;$$

The heat transfer coefficient distributions in flow boiling for minichannels h_{TPB} versus heat flux \dot{q}_H for the steady-state conditions are presented in Fig. 9.

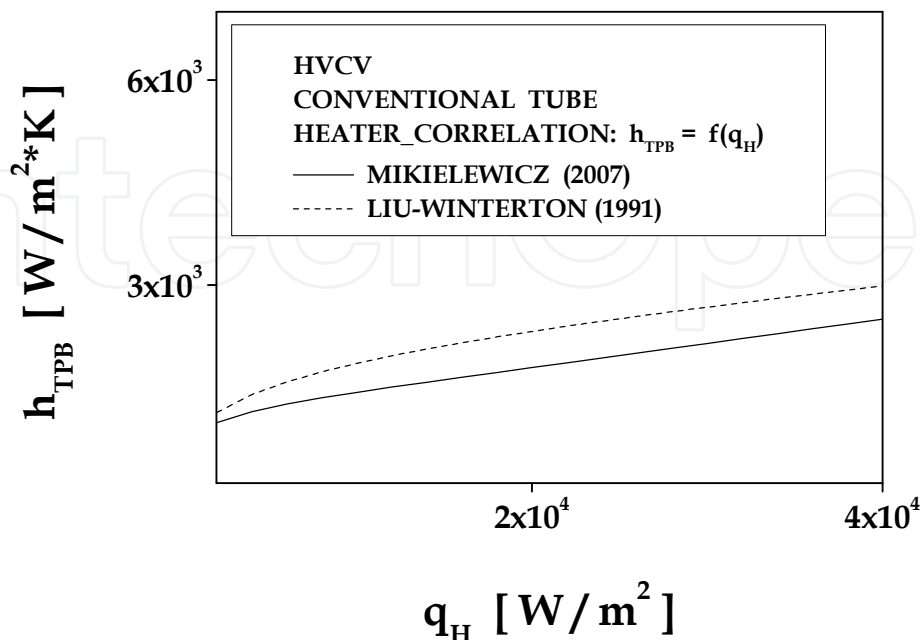


Fig. 9. Heat transfer coefficient h_{TPB} as a function of \dot{q}_H (HVCV).

5. Thermosyphon Loop Heated from the Lower Part of Horizontal Side and Cooled from the Upper Part of Vertical Side (HHCV).

The thermosyphon loop heated from the lower part of horizontal side and cooled from the upper part of vertical side (HHCV) was analyzed for case of two-phase flow in minichannels. A schematic diagram of the analysed thermosyphon loop is shown in Fig. 10. In case of a thermosyphon loop with minichannels, it is necessary to apply some other correlations for void fraction and the local two-phase friction coefficient in the two-phase region, and local heat transfer coefficient for flow boiling and condensation. The following correlations have been used in calculations of the thermosyphon loop with minichannels: the El-Hajal correlation for void fraction (El-Hajal et al., 2003), the Zhang-Webb correlation for the friction pressure drop of two-phase flow in adiabatic region (Zhang & Webb, 2001), the Tran correlation for the friction pressure drop of two-phase flow in diabatic region (Tran et al. 2000), the Mikielewicz (Mikielewicz et al., 2007) and the Saitoh (Saitoh et al., 2007) correlations for the flow boiling heat transfer coefficient for minichannels, the Mikielewicz and the Tang (Tang et al., 2000) correlations for condensation heat transfer coefficient for minichannels.

After integrating momentum equation (2) for the two-phase thermosyphon loop with minichannels (HHCV) can be written in the form

$$\left(\frac{dp}{ds}\right)_{LO} \cdot \left\{ (s_1 - s_0) \cdot \bar{R}_{\langle s_0; s_1 \rangle} + (s_5 - s_1) \cdot \bar{R}_{\langle s_1; s_5 \rangle} + (s_6 - s_5) \cdot \bar{R}_{\langle s_5; s_6 \rangle} + (s_8 - s_6) \right\} + g \cdot (\rho_V - \rho_L) \cdot \left[[(s_3 - s_2) - (s_5 - s_4)] \cdot \bar{\alpha}_{\langle s_1; s_5 \rangle} - (s_6 - s_5) \cdot \bar{\alpha}_{\langle s_5; s_6 \rangle} \right] = 0 ; \quad (18)$$

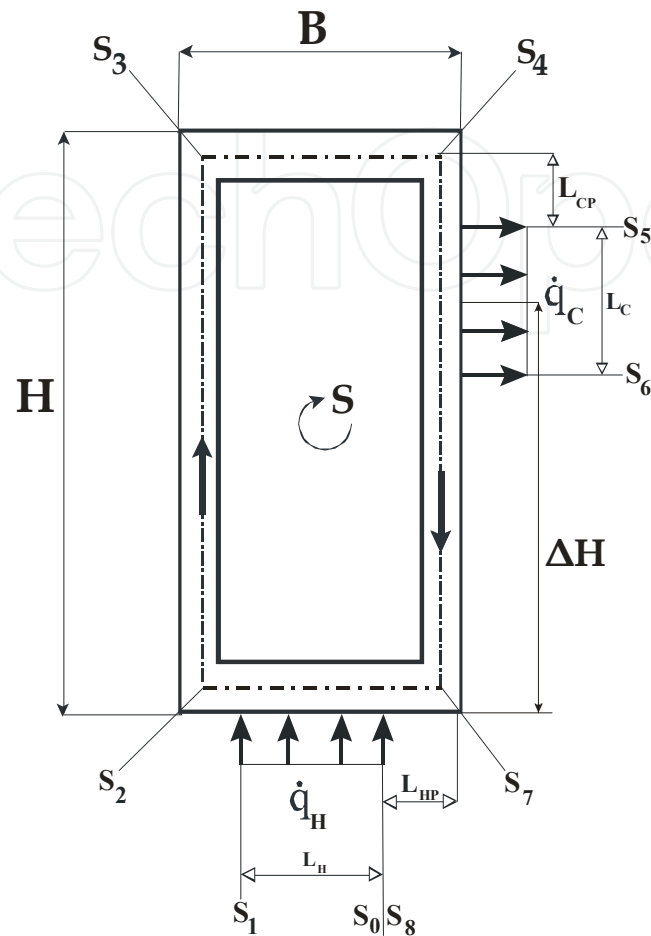


Fig. 10. The scheme of the two-phase thermosyphon loop heated from the lower part of horizontal side and cooled from the upper part of vertical side (HHCV).

The El-Hajal's empirical correlation (El-Hajal et al., 2003) for the void fraction at low pressures is used in calculations

$$\alpha_{\text{HAJAL}} = \frac{\alpha_{\text{HOM}} - \alpha_{\text{STEINER}}}{\ln\left(\frac{\alpha_{\text{HOM}}}{\alpha_{\text{STEINER}}}\right)} ; \quad (19)$$

where

$$\alpha_{\text{STEINER}} = \left(\frac{x}{\rho_V}\right) \times \left\{ \left[1 + 0.12 \cdot (1-x) \right] \cdot \left[\frac{x}{\rho_V} + \frac{1-x}{\rho_L} \right] + \frac{1.18 \cdot (1-x) \cdot [g \cdot \sigma \cdot (\rho_L - \rho_V)]^{0.25}}{\dot{G} \cdot (\rho_L)^{0.5}} \right\}^{(-1)} ;$$

The local two-phase friction coefficient in two-phase adiabatic region was calculated using the Zhang & Webb formula (Zhang & Webb, 2001):

$$\left(\frac{dp}{dl}\right)_{2p}^{Z-W} = \Phi_{L0}^2 \cdot \left(\frac{dp}{dz}\right)_{L0}; \quad (20)$$

$$\Phi_{L0}^2 = (1-x)^2 + 2.87 \cdot (x)^2 \cdot \left(\frac{P}{P_{CRIT}}\right)^{(-1)} + 1.68 \cdot (1-x)^{0.25} \cdot \left(\frac{P}{P_{CRIT}}\right)^{(-1.64)};$$

and the local two-phase friction coefficient in two-phase diabatic regions was calculated using the Tran formula (Tran et al., 2000):

$$\left(\frac{dp}{dl}\right)_{2p}^{TRAN} = \Phi_{L0}^2 \cdot \left(\frac{dp}{dz}\right)_{L0}; \quad (21)$$

$$\Phi_{L0}^2 = 1 + (4.3 \cdot Y^2 - 1) \cdot [N_{CONF} \cdot (x)^{0.875} \cdot (1-x)^{0.875} + (x)^{1.75}];$$

$$N_{CONF} = \frac{\left[\frac{\sigma}{g \cdot (\rho_L - \rho_V)}\right]^{0.5}}{D}; \quad Y = \sqrt{\left(\frac{dp}{dz}\right)_{V0} / \left(\frac{dp}{dz}\right)_{L0}};$$

The mass flux distributions \dot{G} versus heat flux \dot{q}_H were obtained numerically for the steady-state conditions for minichannels, as shown in Fig. 11. The working fluid was distilled water. Two flow regimes can be clearly identified in Fig. 11. GDR - gravity dominant regime and FDR - friction dominant regime.

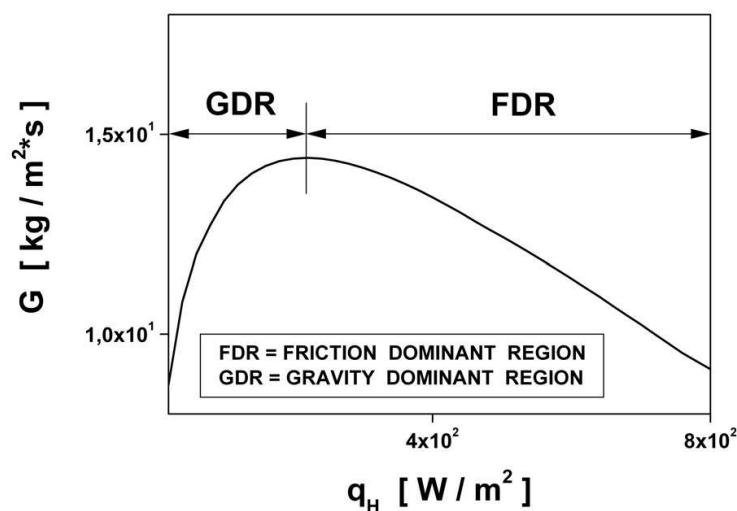


Fig. 11. Mass flux \dot{G} as a function of \dot{q}_H (HHCV), ($L=0.2$ [m], $D=0.002$ [m], $H=0.07$ [m], $B=0.03$ [m], $L_H=L_C=0.025$ [m], $L_{HP}=L_{CP}=0.0001$ [m]).

The gravity dominant regime is characterized by an increase in the flow rate with heat flux \dot{q}_H contrary to the friction dominant regime, which is characterized by a decrease in flow rate with increase in heat flux \dot{q}_H (Vijayan et al., 2005).

5.1 The effect of geometrical parameters on the mass flux distributions.

The effect of the internal diameter tube D on the mass flow rate for the steady-state conditions is presented in Fig. 12. The mass flow rate rapidly increases with increasing internal diameter tube D .

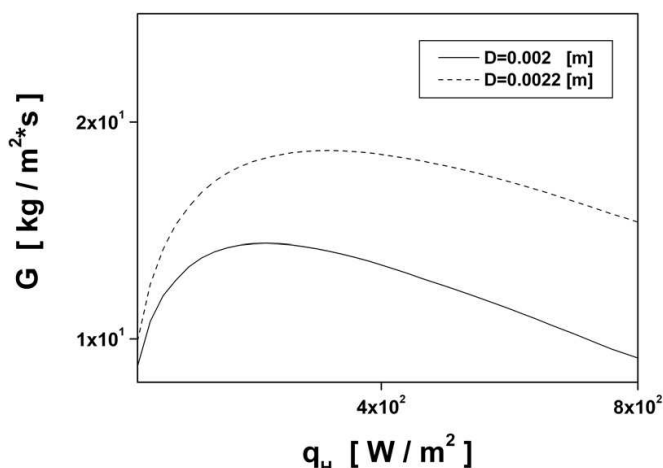


Fig. 12. Mass flux rate \dot{G} as a function of \dot{q}_H with internal diameter tube D as the parameter (HHCV).

The effect of the loop aspect ratio (height H to breadth B) on the mass flow rate for the steady-state conditions is presented in Fig. 13. The mass flow rate increases with increasing H/B aspect ratio, due to the increasing gravitational driving force. The friction force is not changed because the total length of the loop is assumed to be constant.

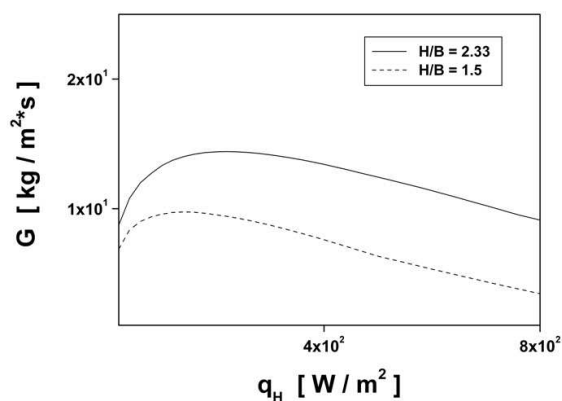


Fig. 13. Mass flux \dot{G} as a function of \dot{q}_H with aspect ratio H/B (height to breadth) as a parameter (HHCV).

The effect of the length of the heated section L_H on the mass flow rate is shown in Fig. 18. The length of FDR- friction dominant regime increases with increasing the length of the heated section L_H .

The effect of the length of preheated section L_{HP} on the mass flux rate was obtained and is demonstrated in Fig. 15. The mass flux rate increases with increasing length of preheated section L_{HP} , due to the decreasing length of insulated section $\langle s_1; s_5 \rangle$.

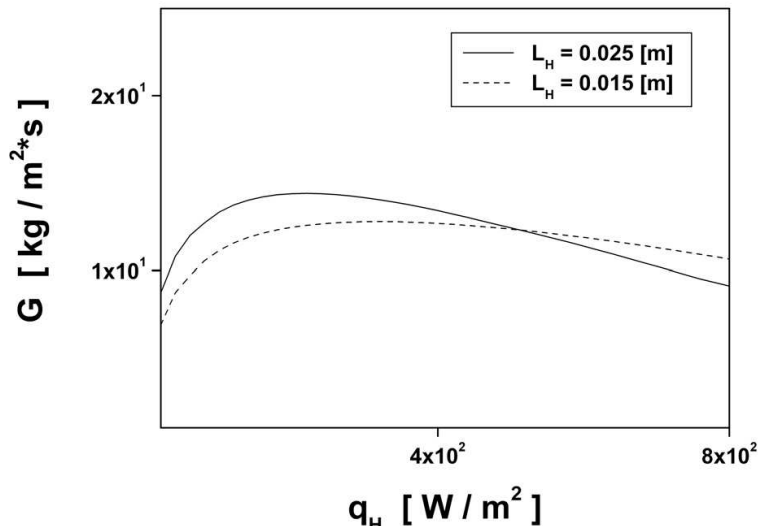


Fig. 14. Mass flux \dot{G} as a function of \dot{q}_H with parameter L_H (HHCV).

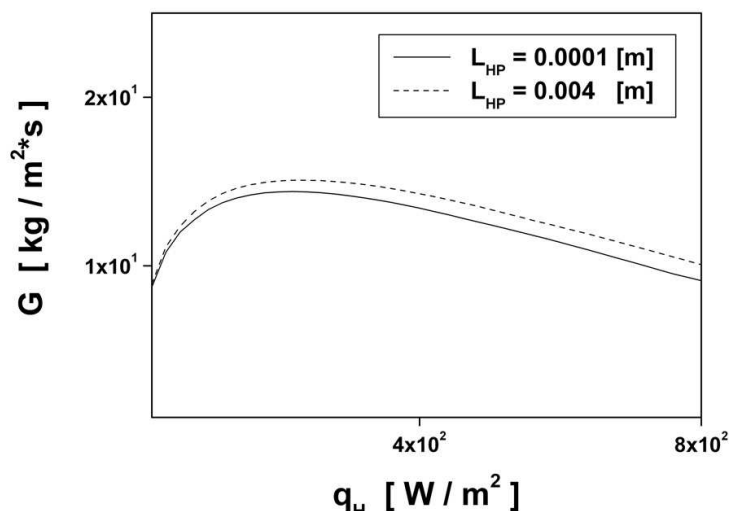


Fig. 15. Mass flux \dot{G} as a function of \dot{q}_H with parameter L_{HP} (HHCV).

The effect of the length of the cooled section L_C on the mass flux rate was also investigated and the results of calculations are presented in Fig. 16. The mass flux rate decreases with increasing length of the cooled section L_C , due to the decreasing gravitational driving force ($\Delta H \downarrow$).

The effect of the length of precooled section L_{CP} on the mass flux rate is shown in Fig. 17. The mass flux rate increases with decreasing length of precooled section L_{CP} due to the decreasing length of insulated section $\langle s_1; s_5 \rangle$ and due to the increasing gravitational driving force ($\Delta H \uparrow$). The decreasing value of the insulated two phase friction pressure

drop $\left(\frac{dp}{ds}\right)_{\langle s_1; s_5 \rangle}^{2p, Friction}$ was caused by the decreasing length of insulated section $\langle s_1; s_5 \rangle$.

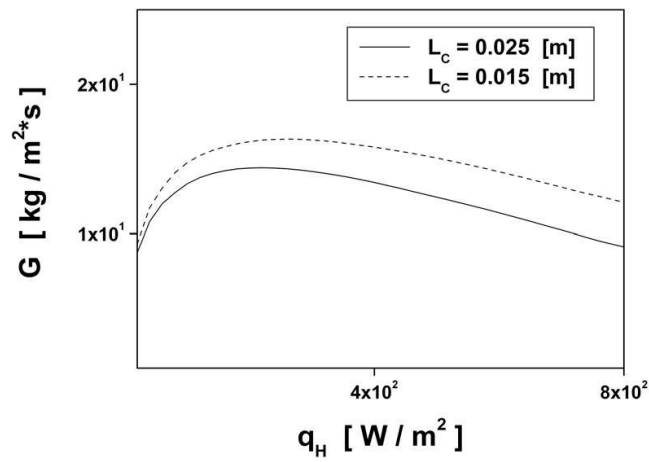


Fig. 16. Mass flux \dot{G} as a function of \dot{q}_H with parameter L_C (HHCV).

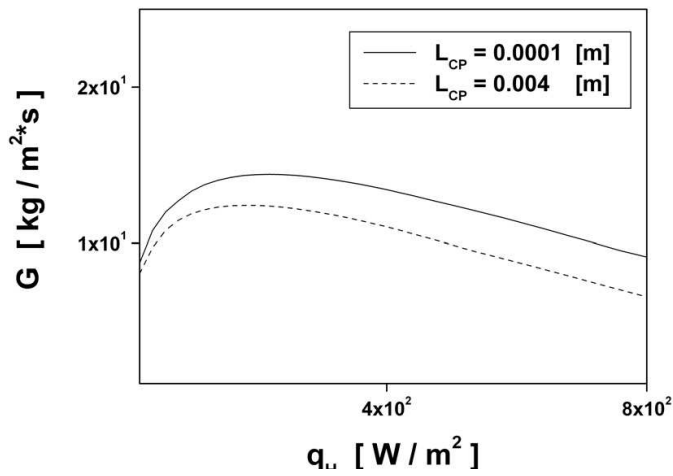


Fig. 17. Mass flux \dot{G} as a function of \dot{q}_H with L_{CP} as a parameter (HHCV)

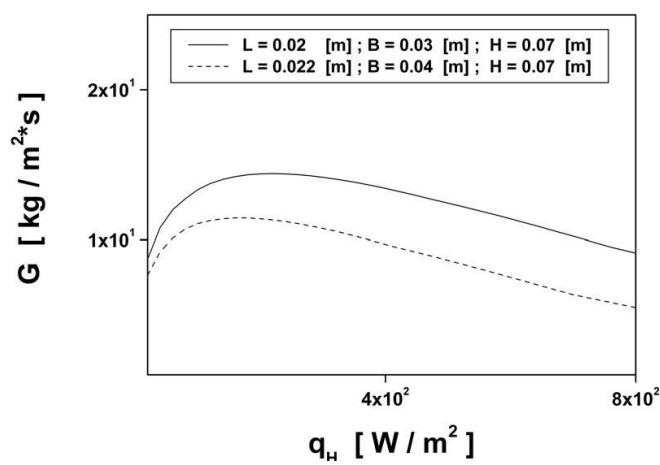


Fig. 18. Mass flux \dot{G} as a function of \dot{q}_H with parameter L (HHCV).

The effect of the total length of the loop L on the mass flow rate is shown in Fig. 18. The mass flow rate decreases with increasing total length of the loop L , due to the increasing frictional pressure drop. The gravitational pressure drop is not changed because the difference of height ΔH of the loop is constant.

5.2 The distributions of the heat transfer coefficient in flow boiling.

The heat transfer coefficient for flow boiling in minichannels was calculated using the Mikielewicz formula Eq. (16) with some modifications concerning the two-phase flow in minichannels, such as:

$$R_{M-S} = \left[1 + 2 \cdot \left(\frac{1}{f_1} - 1 \right) \cdot x \cdot (N_{CONF})^{(-1)} \right] \cdot (1-x)^{\frac{1}{3}} + x^3 \cdot \frac{1}{f_{1z}} ; \quad (22)$$

The heat transfer coefficient for flow boiling in minichannels was also calculated using the Saitoh formula (Saitoh et al., 2007).

$$h_{TPB}^{SAITOH} = E \cdot h_{REF} + S \cdot h_{POOL} ; \quad (23)$$

where

$$h_{POOL} = 207 \cdot \left(\frac{\lambda_L}{d_b} \right) \cdot \left(\frac{q \cdot d_b}{\lambda_L \cdot T_{SAT}} \right)^{0.745} \cdot \left(\frac{\rho_G}{\rho_L} \right)^{0.581} \cdot (Pr_L)^{0.533} ;$$

$$h_{REF} = \begin{cases} (Nu)_{LAM} \cdot \left(\frac{\lambda_L}{D} \right) ; & \text{LAM} \\ 0.023 \cdot (Re_L)^{\frac{4}{5}} \cdot (Pr_L)^{0.4} \cdot \left(\frac{\lambda_L}{D} \right) ; & \text{TUR} \end{cases}$$

$$E = 1 + \frac{\left(\frac{1}{X} \right)^{1.05}}{1 + (We_V)^{(-0.4)}} ; (Re_V) = \frac{\dot{G}_V \cdot D}{\mu_V} ; (Re_L) = \frac{\dot{G}_L \cdot D}{\mu_L} ;$$

$$(We_V) = \frac{\dot{G}_V \cdot D}{\sigma \cdot \rho_V} ; S = \frac{1}{1 + 0.4 \cdot \left[(10^{(-4)}) \cdot (Re_{TP}) \right]^{1.4}} ; d_b = 0.51 \cdot \left(\frac{2 \cdot \sigma}{g \cdot (\rho_L - \rho_V)} \right)^{0.5} ;$$

$$\dot{G}_V = \dot{G} \cdot x ; \dot{G}_L = \dot{G} \cdot (1-x) ; (Re_{TP}) = (Re_L) \cdot (F)^{1.25} ; (Re_L) = \frac{\dot{G}_L \cdot D}{\mu_L} ;$$

$$X = \left(\frac{1-x}{x} \right)^{0.9} \cdot \left(\frac{\rho_G}{\rho_L} \right)^{0.5} \cdot \left(\frac{\mu_L}{\mu_G} \right)^{0.1} \quad \text{for } \begin{cases} (Re_L) > 1000 \\ (Re_G) > 1000 \end{cases} ;$$

$$C_V = 0.046 ; C_L = 16 ;$$

$$X = \left(\frac{C_L}{C_V} \right)^{0.5} \cdot (Re_G)^{(-0.4)} \cdot \left(\frac{G_L}{G_V} \right)^{0.5} \cdot \left(\frac{\rho_V}{\rho_L} \right)^{0.5} \cdot \left(\frac{\mu_L}{\mu_V} \right)^{0.5} \quad \text{for } \begin{cases} (Re_L) < 1000 \\ (Re_V) > 1000 \end{cases} ;$$

The heat transfer coefficient for flow boiling in minichannels h_{TPB} versus heat flux \dot{q}_H is presented in Fig. 19.

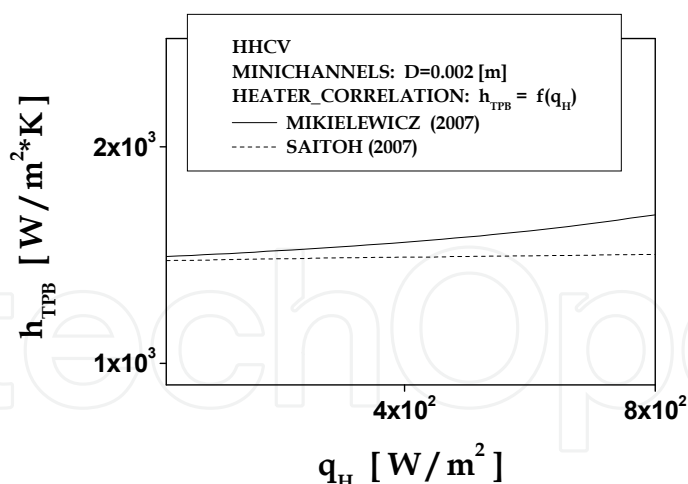


Fig. 19. Heat transfer coefficient α_{TPB} as a function of \dot{q}_H (HHCV).

5.3 The heat transfer coefficient for condensation.

The heat transfer coefficient in condensation for minichannels was calculated using the general Mikielwicz formula Eq. (16). The term which describes nucleation process in that formula was neglected.

The heat transfer coefficient for condensation in minichannels was also calculated using the modified Tang formula (Tang et al., 2000)

$$h_{TPC}^{TANG} = (Nu) \cdot \left(\frac{\lambda_L}{D} \right) \cdot \left[1 + 4.863 \cdot \frac{\left((-x) \cdot \ln \left(\frac{P_{SAT}}{P_{CRIT}} \right) \right)^{0.836}}{(1-x)} \right]; \tag{24}$$

The heat transfer coefficient for condensation in minichannels h_{TPC} versus heat flux \dot{q}_C is presented in Fig. 21.

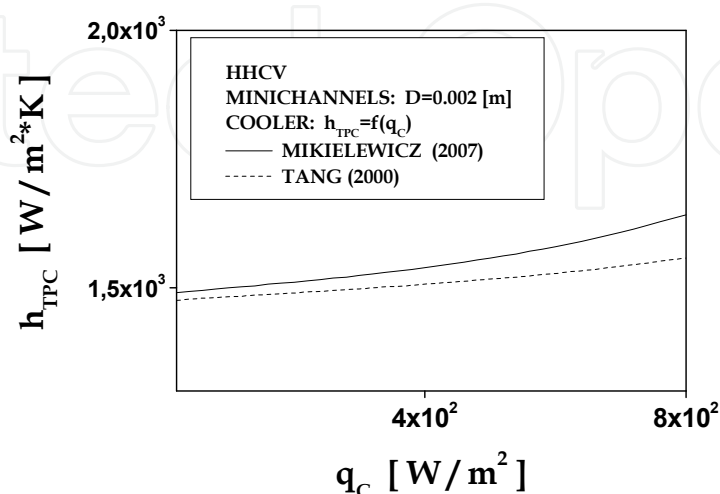


Fig. 20. Heat transfer coefficient h_{TPC} as a function of \dot{q}_C (HHCV).

6. Conclusions

The presented variants (HHCH, HVCV, HHCV) of the thermosyphon loop can be analyzed using the conservation equations of mass, momentum and energy based on a generalized model of the thermosyphon loop. We have found a new and effective numerical method to solve the problem for the onset of motion in a fluid from the rest.

Our studies demonstrate that the best choice of the presented variants depends on specific technical conditions. The increasing integration of electronic systems requires improved cooling technologies. Because the progress in electronic equipment is due to the increased power levels and miniaturization of devices, the traditional cooling techniques are not able to cool effectively at high heat fluxes, so the thermosyphon cooling is an alternative technology allowing to dissipate high local heat fluxes.

The application of the complexity analysis for the various variants of a generalized model of the thermosyphon loop can support development of an alternative cooling technology.

The results show that the one-dimensional two-phase separate flow model can be used to describe heat transfer and fluid flow in the thermosyphon loop for conventional tube as well as minichannels. The Stomma correlation (Stomma, 1979) for void fraction, the Friedel correlation (Friedel, 1979) for the friction pressure drop of two-phase flow in adiabatic region, the Müller-Steinhagen & Heck correlation (Müller-Steinhagen & Heck, 1986) for the friction pressure drop of two-phase flow in diabatic region and the Mikielewicz correlation (Mikielewicz et al., 2007) for the flow boiling heat transfer coefficient in conventional channels can be used to evaluate the thermosyphon loop.

In order to evaluate the thermosyphon loop with minichannels the following correlations such as the El-Hajal correlation (El-Hajal et al., 2003) for void fraction, the Zhang-Webb correlation (Zhang & Webb, 2001) for the friction pressure drop of two-phase flow in adiabatic region, the Tran correlation (Tran et al., 2000) for the friction pressure drop of two-phase flow in diabatic region and the Mikielewicz correlation (Mikielewicz et al., 2007) for the heat transfer coefficient in evaporator, the Mikielewicz correlation for condensation heat transfer coefficient in minichannels, can be used in calculations.

The distribution of the mass flux against the heat flux approaches a maximum and then slowly decreases for minichannels, and two flow regimes can be clearly identified: GDR-gravity dominant regime and FDR – friction dominant regime as shown in Fig. 2.

The effect of geometrical parameters on the mass flux distributions was obtained numerically for the steady-state conditions as presented in Figs. 12-18. The mass flow rate increases with the following parameters: (a) increasing of the internal tube diameter, (b) increasing H/B aspect ratio, (c) decreasing length of preheated section L_{HP} , (d) decreasing length of cooled section L_C , (e) decreasing length of precooled section L_{CP} , (f) decreasing total length of the loop L . Fig. 19 and Fig. 20 respectively show that for minichannels the heat transfer coefficient in flow boiling increases with an increasing of the heat flux and the heat transfer coefficient in condensation against the heat flux approaches a maximum and then slowly decreases.

Future trends and developments in the application of mini-loops should be focused on employing complex geometries, such as parallel mini-channels, in order to maximize the heat transferred by the systems under condition of single- and two phase flows. Moreover, the transient analysis should be developed in order to characterize the dynamic behaviour of single- and two phase flow for different combination of boundary conditions. The next

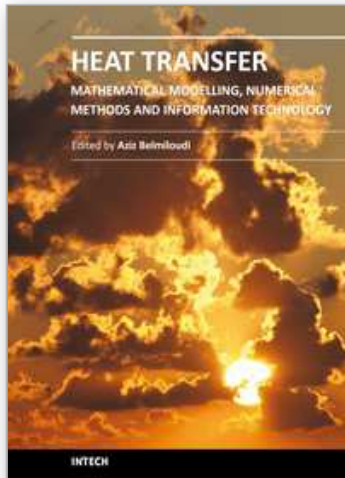
design-step should also be the experimental verification of the theoretical models of thermosyphon loops with minichannels.

7. References

- Bieliński, H.; Mikielwicz, J. (1995). Natural Convection of Thermal Diode., *Archives of Thermodynamics*, Vol. 16, No. 3-4.
- Bieliński, H.; Mikielwicz, J. (2001). New solutions of thermal diode with natural laminar circulation., *Archives of Thermodynamics*, Vol. 22, pp. 89-106.
- Bieliński, H.; Mikielwicz J. (2004). The effect of geometrical parameters on the mass flux in a two phase thermosyphon loop heated from one side., *Archives of Thermodynamics*, Vol. 29, No. 1, pp. 59-68.
- Bieliński, H.; Mikielwicz J. (2004). Natural circulation in two-phase thermosyphon loop heated from below., *Archives of Thermodynamics*, Vol. 25, No. 3, pp. 15-26.
- Bieliński, H.; Mikielwicz, J. (2005). A two-phase thermosyphon loop with side heating, *Inżynieria Chemiczna i Procesowa.*, Vol. 26, pp. 339-351 (in Polish).
- Chen, K. (1988). Design of Plane-Type Bi-directional Thermal Diode., *ASME J. of Solar Energy Engineering*, Vol. 110.
- Churchill, S.W. (1977). Friction-Factor Equation Spans all Fluid Flow Regimes., *Chem. Eng.*, pp. 91-92.
- El-Hajal, J.; Thome, J.R. & Cavalini A. (2003). Condensation in horizontal tubes, part 1; two-phase flow pattern map., *Int. J. Heat Mass Transfer*, Vol. 46, No. 18, pp. 3349-3363.
- Friedel, L. (1979). Improved Friction Pressure Drop Correlations for Horizontal and Vertical Two-Phase Pipe Flow., Paper No. E2, European Two-Phase Flow Group Meeting, Ispra, Italy.
- Greif, R. (1988). Natural Circulation Loops., *Journal of Heat Transfer*, Vol. 110, pp. 1243-1257.
- Liu, Z.; Winterton, R.H.S. (1991). A general correlation for saturated and subcooled flow boiling in tubes and annuli, based on a nucleate pool boiling equation. *Int. J. Heat Mass Transfer*, Vol. 34, pp. 2759-2766.
- Madejski, J.; Mikielwicz, J. (1971). Liquid Fin - a New Device for Heat Transfer Equipment, *Int. J. Heat Mass Transfer*, Vol. 14, pp. 357-363.
- Mertol, A.; Greif, R. (1985). A review of natural circulation loops., In: *Natural Convection: Fundamentals and Applications*, pp. 1033-1071, 1985.
- Mikielwicz, D.; Mikielwicz, J. & Tesmar J. (2007). Improved semi-empirical method for determination of heat transfer coefficient in flow boiling in conventional and small diameter tubes., *Inter. J. Heat Mass Transfer*, Vol. 50, pp. 3949-3956.
- Mikielwicz J. (1995). Modelling of the heat-flow processes., *Polska Akademia Nauk Instytut Maszyn Przepływowych, Seria Ciepłne Maszyny Przepływowe*, Vol. 17, Ossolineum.
- Misale, M.; Garibaldi, P.; Passos, J.C.; Ghisi de Bitencourt, G. (2007). Experiments in a Single-Phase Natural Circulation Mini-Loop., *Experimental Thermal and Fluid Science*, Vol. 31, pp. 1111-1120.
- Müller-Steinhagen, H.; Heck, K. (1986). A Simple Friction Pressure Drop Correlation for Two-Phase Flow Pipes., *Chem. Eng. Process.*, Vol. 20, pp. 297-308.
- Ramos, E.; Sen, M. & Trevino, C. (1985). A steady-state analysis for variable area one- and two-phase thermosyphon loops, *Int. J. Heat Mass Transfer*, Vol. 28, No. 9, pp. 1711-1719.

- Saitoh, S.; Daiguji, H. & Hihara, E. (2007). Correlation for Boiling Heat Transfer of R-134a in Horizontal Tubes Including Effect of Tube Diameter., *Int. J. Heat Mass Tr.*, Vol. 50, pp. 5215-5225.
- Stomma, Z., (1979). Two phase flows-pressure drop values determination." IBJ, Warszawa, INR 1819/IX/R/A.
- Tang, L.; Ohadi, M.M. & Johnson, A.T. (2000). Flow condensation in smooth and microfin tubes with HCFC-22, HFC-134a, and HFC-410 refrigerants, Part II: Design equations. *Journal of Enhanced Heat Transfer*, Vol. 7, pp. 311-325.
- Tran, T.N.; Chyu, M.C.; Wambsganss, M.W.; & France D.M. (2000). Two -phase pressure drop of refrigerants during flow boiling in small channels: an experimental investigations and correlation development., *Int. J. Multiphase Flow*, Vol. 26, No. 11, pp. 1739-1754.
- Vijayan, P.K.; Gartia, M.R.; Pilkhwal, D.S.; Rao, G.S.S.P. & Saha D. (2005). Steady State Behaviour Of Single-Phase And Two-Phase Natural Circulation Loops. 2nd RCM on the IAEA CRP ,Corvallis, Oregon State University, USA.
- Zhang, M.; Webb, R.L. (2001). Correlation of two-phase friction for refrigerants in small-diameter tubes. *Experimental Thermal and Fluid Science*, Vol. 25, pp. 131-139.
- Zvirin, Y. (1981). A Review of Natural Circulation Loops in PWR and Other Systems., *Nuclear Engineering Design*, Vol. 67, pp. 203-225.

IntechOpen



Heat Transfer - Mathematical Modelling, Numerical Methods and Information Technology

Edited by Prof. Aziz Belmiloudi

ISBN 978-953-307-550-1

Hard cover, 642 pages

Publisher InTech

Published online 14, February, 2011

Published in print edition February, 2011

Over the past few decades there has been a prolific increase in research and development in area of heat transfer, heat exchangers and their associated technologies. This book is a collection of current research in the above mentioned areas and describes modelling, numerical methods, simulation and information technology with modern ideas and methods to analyse and enhance heat transfer for single and multiphase systems. The topics considered include various basic concepts of heat transfer, the fundamental modes of heat transfer (namely conduction, convection and radiation), thermophysical properties, computational methodologies, control, stabilization and optimization problems, condensation, boiling and freezing, with many real-world problems and important modern applications. The book is divided in four sections : "Inverse, Stabilization and Optimization Problems", "Numerical Methods and Calculations", "Heat Transfer in Mini/Micro Systems", "Energy Transfer and Solid Materials", and each section discusses various issues, methods and applications in accordance with the subjects. The combination of fundamental approach with many important practical applications of current interest will make this book of interest to researchers, scientists, engineers and graduate students in many disciplines, who make use of mathematical modelling, inverse problems, implementation of recently developed numerical methods in this multidisciplinary field as well as to experimental and theoretical researchers in the field of heat and mass transfer.

How to reference

In order to correctly reference this scholarly work, feel free to copy and paste the following:

Henryk Bieliński and Jarosław Mikielwicz (2011). Natural Circulation in Single and Two Phase Thermosyphon Loop with Conventional Tubes and Minichannels, Heat Transfer - Mathematical Modelling, Numerical Methods and Information Technology, Prof. Aziz Belmiloudi (Ed.), ISBN: 978-953-307-550-1, InTech, Available from: <http://www.intechopen.com/books/heat-transfer-mathematical-modelling-numerical-methods-and-information-technology/natural-circulation-in-single-and-two-phase-thermosyphon-loop-with-conventional-tubes-and-minichanne>

INTECH
open science | open minds

InTech Europe

University Campus STeP Ri
Slavka Krautzeka 83/A
51000 Rijeka, Croatia

InTech China

Unit 405, Office Block, Hotel Equatorial Shanghai
No.65, Yan An Road (West), Shanghai, 200040, China
中国上海市延安西路65号上海国际贵都大饭店办公楼405单元

www.intechopen.com

Phone: +385 (51) 770 447
Fax: +385 (51) 686 166
www.intechopen.com

Phone: +86-21-62489820
Fax: +86-21-62489821

IntechOpen

IntechOpen

© 2011 The Author(s). Licensee IntechOpen. This chapter is distributed under the terms of the [Creative Commons Attribution-NonCommercial-ShareAlike-3.0 License](#), which permits use, distribution and reproduction for non-commercial purposes, provided the original is properly cited and derivative works building on this content are distributed under the same license.

IntechOpen

IntechOpen